

This article appeared in a journal published by Elsevier. The attached copy is furnished to the author for internal non-commercial research and education use, including for instruction at the authors institution and sharing with colleagues.

Other uses, including reproduction and distribution, or selling or licensing copies, or posting to personal, institutional or third party websites are prohibited.

In most cases authors are permitted to post their version of the article (e.g. in Word or Tex form) to their personal website or institutional repository. Authors requiring further information regarding Elsevier's archiving and manuscript policies are encouraged to visit:

<http://www.elsevier.com/authorsrights>



Contents lists available at ScienceDirect

NeuroImage

journal homepage: www.elsevier.com/locate/ynimg

fNIRS evidence of prefrontal regulation of frustration in early childhood[☆]

Susan B. Perlman^{a,*}, Beatriz Luna^a, Tyler C. Hein^a, Theodore J. Huppert^b

^a University of Pittsburgh Department of Psychiatry, USA

^b University of Pittsburgh Department of Radiology, USA

ARTICLE INFO

Article history:

Accepted 14 April 2013

Available online 25 April 2013

Keywords:

Frustration

Emotion regulation

fNIRS

Development

Early childhood

Prefrontal cortex

ABSTRACT

The experience of frustration is common in early childhood, yet some children seem to possess a lower tolerance for frustration than others. Characterizing the biological mechanisms underlying a wide range of frustration tolerance observed in early childhood may inform maladaptive behavior and psychopathology that is associated with this construct. The goal of this study was to measure prefrontal correlates of frustration in 3–5-year-old children, who are not readily adaptable for typical neuroimaging approaches, using functional near infrared spectroscopy (fNIRS). fNIRS of frontal regions were measured as frustration was induced in children through a computer game where a desired and expected prize was “stolen” by an animated dog. A fNIRS general linear model (GLM) was used to quantify the correlation of brain regions with the task and identify areas that were statistically different between the winning and frustrating test conditions. A second-level voxel-based ANOVA analysis was then used to correlate the amplitude of each individual's brain activation with measure of parent-reported frustration. Experimental results indicated increased activity in the middle prefrontal cortex during winning of a desired prize, while lateral prefrontal cortex activity increased during frustration. Further, activity increase in lateral prefrontal cortex during frustration correlated positively with parent-reported frustration tolerance. These findings point to the role of the lateral prefrontal cortex as a potential region supporting the regulation of emotion during frustration.

© 2013 Elsevier Inc. All rights reserved.

Introduction

The feeling of frustration, defined as the obstruction to a desired goal, is an everyday experience that is present even in early childhood. Preschool age children are frequently met with the challenges of regulating emotions during frustrating experiences like early bedtimes, off-limits toys, or prohibited desserts. However, outside of the infancy literature, where frustration is hypothesized to be a stable, enduring aspect of temperament (Rothbart et al., 2000; Stifter and Jain, 1996), individual differences in frustration tolerance have been largely understudied. Even less is known about the neural signatures of frustration in childhood, likely a result of difficulties in measuring brain activity during ecologically valid moments of obstructed goals. Mapping the brain correlates of frustration, therefore, has the potential to not only enhance our scientific understanding of this aspect of temperament, but to elucidate the biological mechanisms

involved in the wide range of frustration tolerance observed in early childhood. The following study was aimed at characterizing neural variation in prefrontal cortical response to frustration in preschool subjects during a typically occurring, frustrating incident: the loss of a desired prize.

The importance of understanding the development of frustration is grounded in its relationship to emotion regulation. Several studies in infants have demonstrated reliable relationships between low frustration tolerance and use of adaptive regulatory behaviors during induced frustration in the laboratory (BraungartRieker and Stifter, 1996; Calkins et al., 2002). Extended to the preschool age, one study found that uncontrolled externalizing behavior was predicted by infant frustration tolerance (Aksan et al., 1999). Further, poor emotion regulation related to frustration has the ability to negatively impact preschool children in two critical domains. First, the ages of 3–5 are when children typically transition from a home environment to one of school and peers. General negative reactivity, including frustration, is a hindrance to early school success and peer relationships (Blair, 2002; Blair et al., 2004; Denham et al., 2011). Second, increased frustration and subsequent poor emotion regulation has been linked to childhood and adolescent psychopathology (e.g., oppositional defiant disorder, ADHD). In one longitudinal study, parent and preschool teacher report of problem behavior, including frustration, at age 3

[☆] Author note: The authors wish to thank Lisa Bemis and Nancy Beluk for their assistance with subject recruitment and data collection and analysis. We are grateful to the children and families who volunteered to participate in this study. This research was supported by K01 MH094467 (P.I. Susan Perlman), P50 MH084053 (P.I. David Lewis).

* Corresponding author at: University of Pittsburgh, Department of Psychiatry, 121 Meyran Ave, Pittsburgh, PA 15215, USA. Fax: +1 412 383 8336.

E-mail address: Perlmansb2@upmc.edu (S.B. Perlman).

led to a 50% rate of behavior problems and school difficulties at age 6 (Campbell et al., 1986). By age 9, 48% of those with this problem behavior met criteria for an externalizing disorder (Campbell and Ewing, 1990) and many reported social and academic difficulties in adolescence (Campbell, 1995). Thus, research into the early development of this dimension of temperament could potentially inform our understanding of maladaptive behavior predicting school problems and psychopathology.

Few studies have directly probed the neural circuitry underlying frustration, however potential neural mechanisms for the experience of a blocked goal can be inferred from the reward literature. One study in adults found that the omission of the receipt of a reward led to decreased ventral striatum activation paired with increased activation in the right anterior insula and ventral prefrontal cortex (Abler et al., 2005). In contrast, another adult study indicated decreased activation of the ventral prefrontal cortex during omission of anticipated reward receipt (Knutson et al., 2001). From an individual differences point of view, Siegrist and colleagues (Siegrist et al., 2005) found that adults with a high susceptibility to social frustration experienced hyperactivation of the medial prefrontal, anterior cingulate, and dorsolateral prefrontal cortices during omission of reward. An additional, recent, multi-modal imaging study found robust reward related activation in the middle frontal gyrus, which was partly explained by individual sensitivity to reward (Heinzel et al., 2013). Thus, it appears that various regions of the prefrontal cortex might be key components of a network involved in the biological basis of frustration regulation, but the specific manner in which they support this aspect of temperament remains unknown.

While neural circuitry related to reward processing can be extrapolated to frustration in adults, very few studies have focused on these questions in child populations. Further, we are unaware of any studies that have probed the brain bases of individual differences in frustration in an early childhood sample; the age at which excessive frustration can be reliably identified as a risk factor for school problems and psychopathology (Campbell, 1995; Campbell and Ewing, 1990; Denham et al., 2002, 2003; Egger et al., 2006; Wakschlag and Keenan, 2001). The current study sought to investigate prefrontal cortical activity as a mechanism for frustration in preschool children. We employed functional near-infrared spectroscopy (fNIRS), which uses near-infrared light to measure the oxygenated and deoxygenated hemoglobin concentrations related to the neural activity in cortical areas of the brain (Gervain et al., 2011). This technique, which has been reliably used in infant and child research (Aslin and Mehler, 2005), allowed us to monitor changes in blood flow to the prefrontal cortex during an ecologically valid, child frustration task. We hypothesized increased activation in the lateral prefrontal cortex during incidents of frustration. Further, we expected this increase in activation to correlate with individual differences in frustration tolerance, however, given the lack of previous studies on the neural basis of frustration, the direction of that correlation was not easily predictable. On the one hand, it's possible that children with a low frustration tolerance may be less able to engage the lateral prefrontal cortex, which may prevent them from adept emotion regulation. On the other hand, children with a low frustration tolerance, but who are still within the normal range of emotional functioning, may require hyperactivation of the lateral prefrontal cortex during frustration in order to galvanize the brain's emotion regulation circuit and further engage them in a frustrating situation. We predicted, given the high level of emotional functioning in a sample chosen to be free of psychopathology, that increased activation in the lateral prefrontal cortex would correlate positively with frustration tolerance.

Materials and methods

Subjects

Subjects were 22 3–5-year-old children (mean age 4 years 6 months, range 36–77 months) recruited from the local community

through paper and internet advertisements. Twelve male and 10 female subjects were identified by their parents/guardians as 59% Caucasian and 41% African American. All subjects were in good physical health and were reported to have no history of any psychiatric disorder and no history of bipolar disorder, major depression, psychosis, autism spectrum disorders, or mental retardation in a first-degree relative. From this sample, data from five children were eliminated from the study due to equipment error, difficulty in obtaining artifact-free data from the scalp, or child non-compliance. This left a final sample of 17 subjects (9 males/8 females). All recruitment and experimental procedures were approved by the local Institutional Review Board.

fNIRS instrument and analysis

Non-invasive optical imaging was performed with a CW6 real-time fNIRS system (Techen Inc., Milford, MA) as shown in Fig. 1A. In this study, a total of four light source emitter positions each containing a 690 nm (12 mW) and 830 nm (8 mW) laser light and eight detectors were used. The inter-sensor distance was 3.2 cm as shown in Fig. 1C. Sensors were mounted into a custom-built head cap constructed from plastic and Velcro, which was comfortably worn by the participant as shown in Fig. 1B. Three-meter-long fiber optic cables connected the head cap to the fNIRS system, which was positioned behind the participant in the back of the room. For each participant, the fNIRS head cap was positioned according to the international 10–20 coordinate system with the inferior medial corner of the probe at position FpZ as shown in Fig. 1. The probe extended over Brodmann area 10 (ventrolateral prefrontal cortex) and area 46 (dorsolateral prefrontal cortex) on each hemisphere. Once the fNIRS instrument was securely and comfortably placed upon the subject's head, they were seated at a child size desk. Upon the desk was a touchscreen computer, designed to present the task and record responses. One experimenter was seated at the desk next to the subject in order to guide him/her through the task. A second experimenter remained behind the subject in order to control and monitor the fNIRS instrument. On average, the total fNIRS setup time to place the head cap was around 5 min.

During the study, the fNIRS data was collected at a sample rate of 4 Hz through a custom-built data acquisition interface as described in (Abdelnour and Huppert, 2009). This software allowed fNIRS signals (oxy- and deoxy-hemoglobin) to be visualized in real-time during collection. The operator was also able to add comments to the data in real-time to indicate subject events such as motion or distractions. The timing for the stimulus presentation through the Eprime (Psychology Software Tools, Sharpsburg, PA) program was recorded in sync with the fNIRS data through an analog signal from the computer LPT port.

Analysis of the fNIRS data in this study was based on a general linear model similar to the approach commonly applied to functional MRI data (see Fig. 2). First, optical channels with very poor signal due to poor contact with the head were removed from the analysis during preprocessing. These signals were defined as having a temporal variance significantly greater than the median variance of the remaining channels at significance ($p < 0.05$). If one of the two optical wavelengths was poor for a given source-detector pair, then both wavelengths had to be removed from the analysis. On average 7.1% of the channels were removed across subjects. Any periods of time containing motion or other distractions that had been manually marked by the fNIRS operator during data collection were discarded. The remaining raw optical signals were motion corrected using a motion-correction algorithm based on a spline interpolation. In brief, an independent component analysis (ICA) of the data from each scan was performed. In general, the data transformation according to ICA results in the projection of strong motion artifacts onto one or a few of the components. For each independent component, the discrete 1st-order temporal derivative of the data was taken and the resulting time trace was

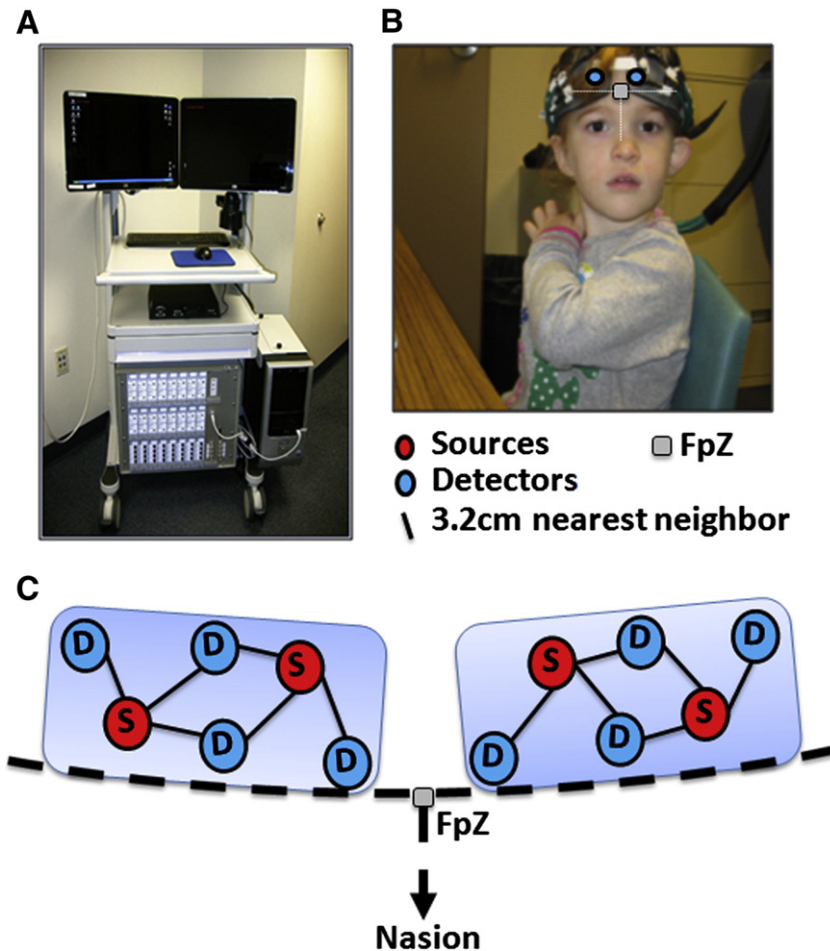


Fig. 1. A. Image of the portable CW6 fNIRS instrument (TechEn Inc., Milford, MA USA) used in this study. B. Image of a child demonstrating the placement of the fNIRS cap. C. Schematic of the fNIRS cap layout design.

Z-transformed ($Z(t) = Y(t)/\sqrt{(Y(t)-Y)^2}$). Both spike and shift types of motion-artifacts are identified as quick jumps in the data as defined by the outliers ($p < 0.01$) in this Z-transformed temporal derivative. A cubic spline interpolation was then used to replace the identified outlier time-points affected by the motion for each independent component with time-points before and after the artifact. This is similar to the spline motion-correction scheme described in Scholkmann et al. (2010). Previous work by Cooper et al. (2012) had found that the spline motion-correction approach produced the highest average decrease in mean squared error. The signal was then re-integrated and these corrected independent components were then reconstructed back to the original channel space. On average (median) the motion correction algorithm removed 9.1% [range 6.8–12.2%] and 8.1% [6.1–11.4%] of the variance off the optical density measurements at 690 nm and 830 nm respectively. The median kurtosis (“peakedness”) of the data was lowered by 5.6% and 4.5% by the motion correction algorithm for 690 nm and 830 nm respectively. This change is rather small and indicated that most of this data did not have significant motion. A 15% or higher change in the kurtosis metric as the result of motion correction was only found in a small fraction (12.8%; 11 of 86) of all the data files. Following motion-correction, data was converted to optical density changes and down-sampled to 1 Hz. It should be noted that for fNIRS studies, motion artifacts arise from movement of the head cap relative to the head and were greatly reduced by construction of a comfortable, yet tight-fitting head cap design that minimized probe slippage. Since

the cap was affixed to the child’s head, the child was able to move around in the context of interacting with the computer monitor and the task without producing artifacts on the fNIRS data.

After motion-correction preprocessing, first level statistical analysis was done using a canonical general linear model (Ye et al., 2009). This approach is identical to the general linear model approach used in most fMRI studies (e.g., Friston, 2007). A hemodynamic response based on a gamma-variant function with parameters taken from published fMRI methods (Friston, 2007) was used for this study and convolved with the boxcar timing of the stimulus epochs. High-pass filtering is done inside the GLM model by projection of drift (pre-whitening) from both the data and design matrix using a high-pass filtering discrete cosine transform matrix (>0.016 Hz pass-band; see Fig. 2) (e.g. $S \cdot Y = S \cdot X \cdot \beta$ where Y is the data vector, X is the GLM design matrix, β is the coefficients of the model describing the amplitude of brain activity, and S is the filtering matrix). This approach, which is the method of filtering used in fMRI analysis (e.g. SPM8) and within the NIRS-SPM program (Ye et al., 2009), is preferable to a direct filtering on the data alone, which can over-correct and remove brain activation in the context of the longer-duration tasks used in this study. Since this filter is applied to both the data and the design matrix (e.g. multiplies both sides of the linear model), this approach prevents over-correction in the case where the stimulus timing is close to the effective stop-band of the filter. A restricted maximum likelihood (ReML) model was used to solve the regression model using an iteratively weighted least-squares (e.g. the Gauss–Markov equation) (Friston, 2007). The

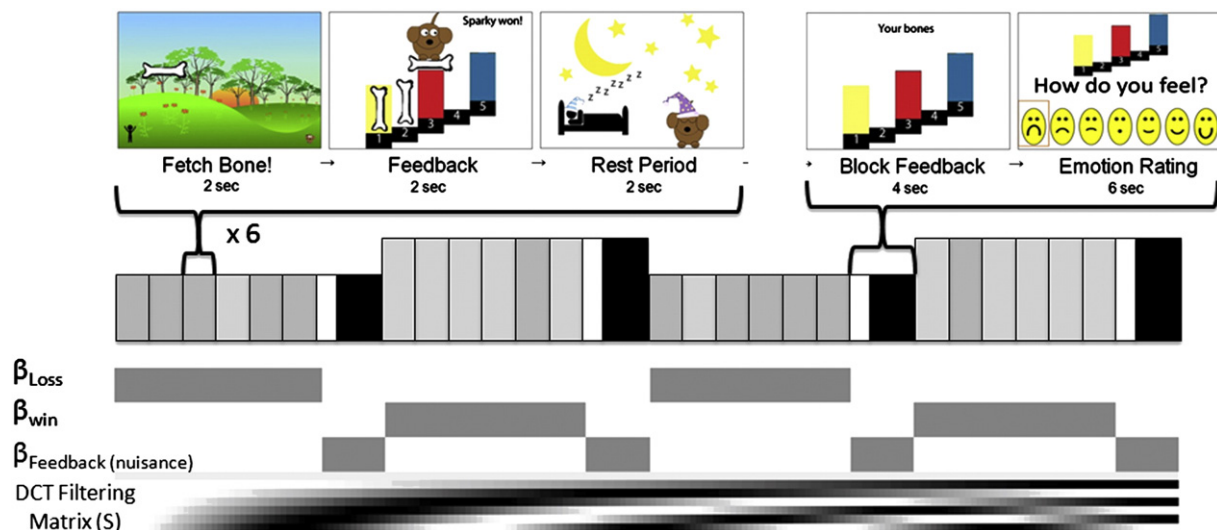


Fig. 2. Visual representation of the FETCH task along with the design matrix of the general linear model.

magnitude of changes (e.g. coefficients in the GLM regression model; β as denoted in the equation above) was estimated for each optical source-detector pair and for each task condition. The general linear model design is shown in Fig. 2, two functional contrasts (β_{win} and β_{Loss}) and a nuisance variable ($\beta_{feedback}$) representing the average activity over the win, loss, and feedback blocks respectively. The functional contrast was defined as the difference between the win and loss coefficients in the GLM.

In order to visualize the maps of brain activation, the optical images were reconstructed from the estimated GLM model coefficients established on a template brain from an age-matched subject as described in Abdelnour et al. (Abdelnour and Huppert, 2010; Abdelnour et al., 2010). Based on the placement of fNIRS probe relative to the international 10–20 coordinate system, the sensitivity of the optical measurements to the underlying brain was modeled based on the brain anatomy of an age-matched child's MRI data who participated in a previous study (Perlman and Pelphrey, 2010, 2011). This template MRI structural image was segmented into skin, skull, cerebral spinal fluid, and brain tissue layers as previously described in (Abdelnour et al., 2009). A Monte Carlo implementation (Fang and Boas, 2009) of the optical diffusion approximation was used to simulate the optical “forward” model from this template in order to visualize the fNIRS results. Although individual differences in brain anatomy will alter the sensitivity of the fNIRS measurements, previous publications have shown that atlas-based fNIRS analysis still provide a close approximation to individualized models (Custo et al., 2006).

The fNIRS measurement sensitivity model for each subject was inverted using a random-effects inverse model (Abdelnour and Huppert, 2011) to produce an estimate of the brain activation map for each subject and the weighted average of the two subject groups (controls and cussed). In this random-effects model (Abdelnour and Huppert, 2011), the forward models obtained from the simulation model each subject's registration are collected into a single linear matrix operator such that the estimate of each subject's brain activity is the sum of the group average and a random-effects perturbation term for that subject. Thus, instead of performing multiple independent image reconstructions (one for each subject), the larger combined forward model is inverted in order to estimate an image of brain activity that is most simultaneously consistent with all participants' data. This approach was shown to be less susceptible to artifacts and errors introduced by outlier measurements in only a few participants (Abdelnour and Huppert, 2011). A hierarchical statistical model and Restricted

maximum likelihood (ReML) was used (Abdelnour et al., 2010). ReML is an empirical Bayesian method, which is used to provide stabilization of the inverse (image reconstruction) model and for simplified models is mathematically equivalent to an L-curve technique to optimize regularization (Abdelnour et al., 2010). This approach has been widely used in fMRI analysis (Cox, 1996; Friston, 2007) and in the implementation of the similar image reconstruction problem for electroencephalography (EEG) and magnetoencephalography (MEG) within the software SPM-8 (Friston, 2007; Mattout et al., 2006). The use of ReML for fNIRS was described in Abdelnour et al. (Abdelnour and Huppert, 2010). Also of note, our ReML based random-effects image reconstruction method used in this work is very similar to the implementation of the random-effects MEG reconstruction model used in SPM-8 (Mattout et al., 2006).

Finally, the reconstructed oxy- and deoxy-hemoglobin activation maps for each subject were further used in a voxel-based ANOVA regression to identify regions of brain activity that were correlated with the behavioral frustration metrics across the group of subjects. In the voxel-wise ANOVA analysis, the amplitude of brain activity at each voxel was regressed within a fixed effects multi-way ANOVA model (Mathworks Matlab function *anovan.m*; Version 7.13; Release 2011b) with irritability as a factor of interest and age (months) and gender as co-factors of no interest.

Questionnaires

During the fNIRS recordings, the parent/guardian of the subject was seated in the back of the room to fill out the questionnaires. S/he completed the *Child Behavior Questionnaire (CBQ)-Long Form* (Rothbart et al., 2001), an experimentally-validated and commonly used caregiver assessment of 15 dimensions of children's temperament. Our hypotheses focused on the Anger/Frustration dimension of temperament. The parent/guardian completed an additional demographics form.

The Frustrative Emotion Task for Children (FETCH)

Before task performance, subjects were shown three boxes and told that they were going to be playing a game in which they would win a prize from these boxes. Their performance on the game would determine from which box they would be allowed to choose this prize. The large, blue box contained many exciting toys and games that were

attractive to children. The medium, red box contained an assortment of stickers and the small, yellow box contained a single broken crayon. The selection of the disappointing prize box was modeled after previous work using a similar technique to set up the expectation that children would receive their desired prize (Cole, 1986; Saami, 1984).

In the task, subjects competed with Sparky, “a very sneaky dog”, to fetch bones by touching the bone as it appeared on the screen. Unbeknownst to the subject, each trial was fixed where sometimes the child could fetch the bone before Sparky (win trials), but sometimes the Sparky would fetch the bone before the child’s possible reaction time (frustration trials). Win trials were indicated by an animated line drawing depicting the child grabbing the bone and placing it within one of the five prize boxes while frustration trials showed Sparky grabbing the bone and then taking a bone out of a previously won box (see Fig. 2). Five bones had to be accumulated in order to win a prize from the large (blue) box. Children were told that at the end of the game, they would win their prize from the highest box that they would be able to fill. Each six second trial consisted of two seconds in which the bone appeared on the screen for the child to fetch, followed by two seconds of feedback in which a bone was earned or removed, and then a 2-second inter-stimulus interval in which the child was told to rest (Fig. 2). The task was animated and contained engaging sound effects.

Trials were also grouped into *Winning blocks*, designed to induce children into a positive/happy mood, and *Frustration blocks*, designed to induce a negative/frustrated mood. Each *Winning block* contained 5 win trials and 1 frustration trial, allowing children to earn 4 total bones (one less than the amount needed to earn a prize from the big, blue box). Each *Frustration block* contained 5 loss trials and 1 win trial in which children lost all previously earned bones and ended the block with 0 bones. At the end of each block, children were shown their cumulative bones. They were asked to complete an online emotion rating by choosing from a spectrum of seven line drawn faces representing how they were feeling ranging from a negative to a positive mood (see Fig. 2). The full task began with a *Winning block* and alternated between *Winning* and *Frustration blocks* to include five total blocks. In the final *Winning block*, the addition of an extra win trial allowed all children to advance to the blue box and receive their desired prize from the large blue box at the end of the game. Thus, the task contained one more winning block (3 total) than losing blocks (2 total). All children completed a practice version of the task before data was recorded in order to ensure understanding of the objective, ability to use the touch screen, and comprehension of the emotion rating system.

This experimental design does not explicitly include long rest periods in which the child is expected to do nothing. This is done to both reduce the amount of time needed to run the study and to maintain the attention of the child towards the task. Although this experimental design is fairly common with similar fMRI studies in children, this design departs from the conventional block-averaging design and analysis models used in many fNIRS studies. This design allows us to quantify brain regions that differed between the *Winning* and *Frustration blocks* via a statistical test (*T*-test) between the amplitudes of the two blocks within the context of the general linear model. However, because the study was designed to lack a true baseline condition, it is not possible to test for regions that we equally activated in the two conditions relative to a rest condition.

Although this experimental design is not routine for fNIRS research, this approach is well established for fMRI studies and in the context of the general linear model. The reason baseline/rest periods were not included was because previous work with children has noted that motion artifacts were more frequent during periods where children are not given a specific task (Wilcox et al., 2005). Additionally, many fMRI studies compare two task conditions only differing in the psychological construct of interest in order to avoid conflicting results due to visual, auditory, or motor demands. Finally,

this design is employed to minimize the amount of participation time required of restless, young children. Indeed, many children of this age group would lose focus on the task if an additional rest condition were added. To avoid these potential confounds, several previous fMRI studies in children have proposed similar experimental designs, which minimize the need for the children to rest or disengage from the given task (Perlman and Pelphrey, 2010, 2011).

Results

Manipulation check

To ensure that all subjects were motivated to win their prize from the large, blue box, each was asked to list their preferred order of boxes before participation. One hundred percent of subjects declared that the large (blue), followed by the medium (red) and then small (yellow) boxes, would be their preferred order.

The online mood rating corresponded to the type of trial. On a seven point scale assigned to each emotional face, ranging from most negative feelings (1) to neutral (4) to most positive feelings (7), subjects gave a significantly more positive mood rating (mean = 6.85) after the *Winning blocks* than after the *Frustration blocks* (mean = 2.75), indicating that the task was successful in inducing negative mood ($t(15) = 8.17, p < .001$). After receiving their desired prize, subjects were asked open-ended questions about their mood state during task participation. One hundred percent reported positive feelings during *Winning blocks* (e.g. “good”, “happy”), 82% reported negative feelings during *Frustration blocks* (e.g. “sad”, “mad”, “bad”), and 70% reported being angry with Sparky when he was taking their bones away. One hundred percent of children reported overall enjoyment of the game.

Neural activity contrast between winning and frustration blocks

The NIRS data was analyzed using the general linear model and reconstructed to brain activation images as detailed in the previous section. The effect size of the activation pattern for each of the optical measurement pairs is shown in Fig. 3 for the contrast between *Winning* and *Frustration blocks*. In this image, each disk corresponds to a measurement pair (one source-detector combination) and the color of the disk indicates the effect size (*T*-statistic) across the group of subjects. Three of the optical measurements pairs on the right hemisphere located around the international 10–20 coordinate of AF8, F6, and F8 (approximately Brodmann areas 45/46) showed significant ($p < 0.05$; corrected) increased oxy-hemoglobin concentrations between the *Winning* versus *Frustration blocks* (Fig. 3a). A single optical channel closest to the AF7 point in the 10–20 coordinate on the left medial frontal cortex (approximately BA 10/46) also showed greater activation during the *Winning block*. A channel between T7 and C5 on the left temporal cortex showed significantly higher ($p < 0.05$) activation during the *Frustration block* compared to the *Winning block*. Deoxy-hemoglobin activation maps (Fig. 3b) showed similar regions significantly increased concentrations between the *Winning* versus *Frustration blocks*. Three channels in the right temporal hemisphere around AF8, F6, and F8 (2 of 3 overlapping with those channels activated in oxy-hemoglobin) and two channels in the left frontal hemisphere near Fp1 and AF7 (1 of 2 overlapping with those activated in oxy-hemoglobin) were observed ($p < 0.05$). In these channels, both oxy-hemoglobin and deoxy-hemoglobin concentrations were observed to be higher during the *Winning blocks* compared to *Frustration*. This is somewhat inconsistent with the expectation of the typically hyperemic hemodynamic response (e.g. increase in oxy-hemoglobin and a decrease in deoxy-hemoglobin). It is possible that this inconsistency could represent cross-talk between the two hemoglobin chromophores in the optical measurement. The issue of hemoglobin cross-talk has been previously addressed by Strangman et al.

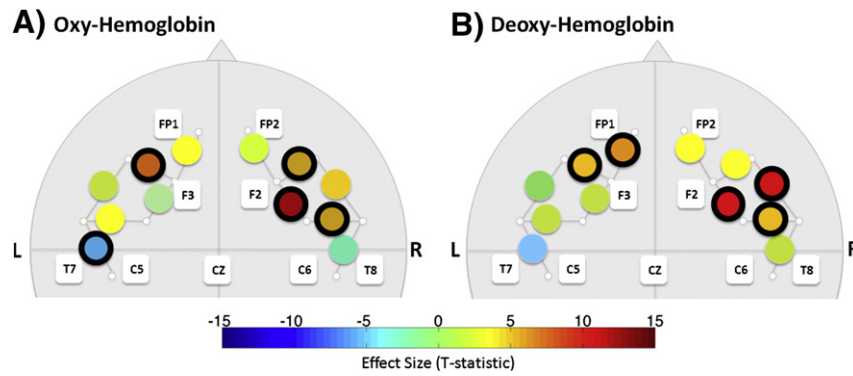


Fig. 3. Brain activity contrast for the group-level hemoglobin signals during the Winning blocks minus the Frustration blocks. Each disk indicates the effect size (T-statistic) for the comparison of the two conditions in the general linear model for each fNIRS source-detector pair. Individual optical measurements that met $p < 0.05$ [corrected] significance are outlined with dark lines. Each disk is drawn at the center of the location on the head sampled by that measurement pair. The approximate locations of the closest international 10-20 coordinates to the fNIRS probe are shown. Oxy- and deoxy-hemoglobin signals are shown in panels A and B respectively.

(2003), who suggested that using the measurement wavelength pair of 690 nm and 830 nm was one of several wavelength combinations that reduced this cross-talk error. However, their modeling approach only specifically looked at the reduction of cross-talk in measurements from the adult head, and thus, cross-talk at these wavelengths could still possibly be an issue in children or infant studies. An alternative interpretation is that the observed increases in both oxy- and deoxy-hemoglobin is physiological and represents a difference in the blood flow and oxygen metabolism coupling in children compared to the expected typical results from adult studies.

Based on the activation maps for each optical measurement pair and the optical sensitivity model constructed from the age-matched MRI template image, estimates of brain activity can be reconstructed to provide better visualization of the NIRS results. The reconstructed brain image from the group of subjects is shown in Fig. 4 for the contrast between Winning and Frustration blocks. We found increased activity (oxy-hemoglobin changes) in the right middle prefrontal cortex (approximately BA 45/46) during Winning blocks compared to Frustration blocks, while activation in the left dorsal prefrontal cortex (approximately BA 10/46) was greater for Frustration blocks compared to Winning blocks. In Fig. 4A, the reconstructed oxy-hemoglobin images for the contrast of Winning minus Frustration blocks is shown on the inflated surface of the age-matched template brain. Deoxy-hemoglobin

images show similar activation patterns to the oxy-hemoglobin images but with slightly reduced effect sizes.

The relationship between temperament and neural frustration

Scores on the Anger/Frustration subscale of the Child Behavior Questionnaire ranged from 1.5 to 6.6 (mean = 4.40) on a seven-point scale, indicating a wide range of parent-reported frustration tolerance in this sample. Anger/Frustration scores were positively correlated with changes in oxygenated hemoglobin [$r(15) = 0.72, p < .001$, two tailed] and with the changes in deoxygenated hemoglobin [$r(15) = 0.48, p < .05$, two tailed] during Frustration blocks in comparison to the Winning blocks in a section of the left DLPFC (See Fig. 5). Greater engagement of DLPFC was associated with higher parent assessment of frustration. No associations were found between the middle PFC with frustration minus winning or for winning minus frustration in either prefrontal region. Fig. 5A shows the brain regions correlated to the frustration score ($p < 0.05$) in the left DLPFC. Fig. 5B shows the scatter plot of the mean amplitude of oxy- and deoxy-hemoglobin contrast from this region-of-interest and frustration scores for each of the 17 subjects. Subjects' online emotion rating scores for both the Winning and Frustration blocks did not correlate with parent reported temperament or with neural frustration.

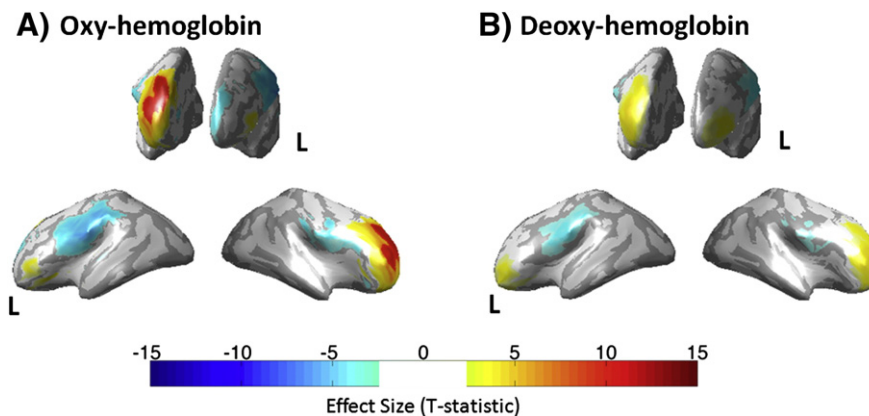


Fig. 4. Reconstructed images of brain activity for the contrast of the Winning blocks minus the Frustration blocks. FNIRS data was reconstructed and displayed using an age-matched template of a brain for visualization purposes. Oxy- and deoxy-hemoglobin signals are shown in panels A and B respectively.

Discussion

General discussion

Using fNIRS during an ecologically-valid, child frustration task, we found increased activation of the middle prefrontal cortex in response to winning and increased activation of the lateral prefrontal cortex during frustration. Further, parent ratings of children's frustration tolerance correlated with increased activation of the lateral prefrontal cortex from rewarding to frustrating moments.

Increased activation of the middle prefrontal cortex during the Winning block can be supported by its well defined role in response to the receipt of reward in adults (Heinzel et al., 2013; Xue et al., 2009), rats (Tzschentke, 2000), and children (May et al., 2004). Most closely related to the current study, a recent publication by Heinzel et al. (2013) employed simultaneous fNIRS and fMRI imaging during a reward paradigm. The authors noted increased activation during the reward period in the same middle frontal gyrus region observed in our study in both the fNIRS and fMRI data. Self reported reward sensitivity, however, was only correlated with fMRI data in this region, which may indicate that fNIRS is not able to penetrate the cortex to the depth of the most reward-sensitive, prefrontal regions. An alternative explanation for these findings can be found in the self-reflection literature. The line drawings of a child representing the subject, which was exclusive to winning trials, may have engaged self-reflection processes that have also been found to be supported by the medial PFC in both adults (Gusnard et al., 2001; Mitchell et al., 2005) and children (Pfeifer et al., 2007) in fMRI studies.

Our hypothesis predicting increased activation of the lateral prefrontal cortex during the event of a blocked goal was supported in the current study. This finding is similar to the reward literature in which subjects activated this region when an anticipated reward was not received (Ablner et al., 2005; Knutson et al., 2001; Siegrist et al., 2005). Another explanation for these findings can be found in the developmental executive function literature. Inhibitory control, which has been tied to emotion regulation in preschool children (Carlson and Wang, 2007), has been tied to activation of the lateral prefrontal cortex in both adult (Herrmann et al., 2005) and child (Inoue et al., 2012) fNIRS research. Attention/task shifting, another executive function hypothesized to be critical to emotion regulation (Gross, 1998) has been related to the use of the lateral PFC in preschool children through fNIRS (Moriguchi and Hiraki, 2009).

Further, the level of increased activation in the left lateral prefrontal cortex correlated with temperament ratings of child frustration.

Although we predicted increased activation of this region to correlate positively with frustration tolerance, it was unclear if the effect would appear in this direction. On the one hand, children who have a low frustration tolerance could have decreased activation in this area, which could be the root of their low frustration tolerance. On the other hand, children who reach high levels of normal temperamental frustration in their everyday lives, but have not experienced psychopathology, may need to recruit this area in order to regulate their emotions and complete the task. Our results support the latter possibility. These findings (a moderate, positive correlation between temperament and oxygenated/deoxygenated hemoglobin in the lateral prefrontal cortex during frustration) point to the likelihood of the engagement of the lateral prefrontal cortex in an emotion regulation circuit, which is critical for the modulation of frustration, especially in those children who are the most frustrated. Findings indicate the ability to engage this region in emotion regulation at a young age, and point to the possibility that the use of this region, as part of an emotion regulation circuit, may become more efficient as the prefrontal cortex continues to develop (Giedd, 2004; Gogtay et al., 2004; Rakic et al., 1994). Further, maturation of this region may be compromised due abnormal brain maturation in development of psychopathology, which may underlie behavioral regulatory deficits not seen in a normal sample. Future research is planned to assess this effect in clinically irritable children, who experience high levels of frustration in everyday functioning, and may experience decreased ability to recruit the lateral prefrontal cortex in correlation with high levels of psychopathological symptoms.

Limitations

While the results of this study provide new evidence for distinct patterns of activation related to the experiences of reward and frustration in the prefrontal cortex in early childhood, some limitations of this study must be noted. First, fNIRS is a region-of-interest technique that is capable only of imaging the brain at the cortical surface. Thus, we were not able to examine additional, subcortical, brain regions that might play an important role in frustration in early childhood. Reward processing regions, such as the striatum (Delgado et al., 2000; Schultz et al., 1992) and emotional reactivity regions, such as the amygdala (Gallagher and Chiba, 1996; Morris et al., 1996), may form part of a circuit that decreases in efficiency as preschoolers with high frustration tolerance reach middle childhood and adolescence. Future studies are planned to integrate fNIRS and functional magnetic resonance imaging (fMRI) to investigate the relationship

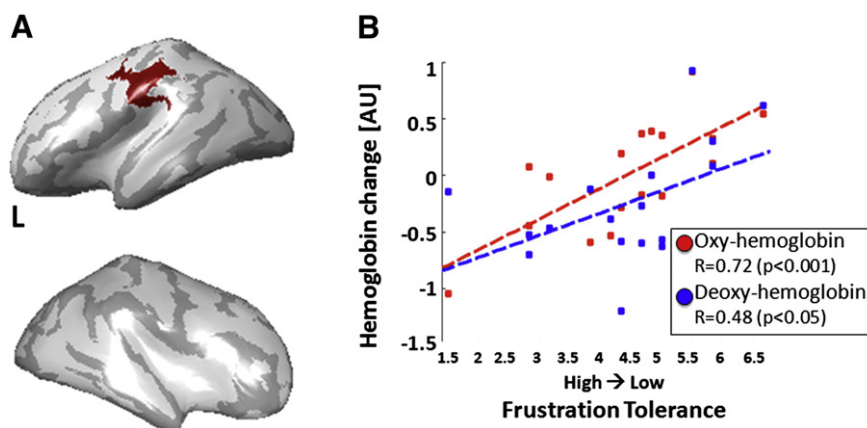


Fig. 5. A. Map of brain regions correlated ($p < 0.05$) with the frustration score in a group-level ANOVA regression model. B. Scatter plot of the mean oxy- and deoxy-hemoglobin from this region-of-interest and frustration score for each of the 17 subjects. Positive correlation is observed between the frustration score and the oxy- and deoxy-hemoglobin contrast of the Frustration minus Winning blocks in the left DLPFC.

between the frontal and subcortical reward circuitry as these brain systems mature. Second, as mentioned previously, we acknowledge issue of hemoglobin cross-talk, which has never been addressed on a child head. This will be an important area for future inquiry. Finally, while the subjects in this study did report a wide range of frustration tolerance, none of them had ever been diagnosed with any form of psychopathology, nor were they impaired in any aspect of social functioning. Future studies including a clinical sample of highly irritable children may shine the light on neural impairments, such as decreased activation in the lateral prefrontal cortex, that would trigger increased frustration and lead to maladaptive social interaction.

References

- Abdelnour, A.F., Huppert, T., 2009. Real-time imaging of human brain function by near-infrared spectroscopy using an adaptive general linear model. *Neuroimage* 46, 133–143.
- Abdelnour, F., Huppert, T., 2010. A random-effects model for group-level analysis of diffuse optical brain imaging. *Biomed. Opt. Express* 2, 1–25.
- Abdelnour, A.F., Huppert, T.J., 2011. A random-effects model for group-level analysis of diffuse optical brain imaging. *Biomed. Opt. Express* 2, 1–25.
- Abdelnour, F., Schmidt, B., Huppert, T.J., 2009. Topographic localization of brain activation in diffuse optical imaging using spherical wavelets. *Phys. Med. Biol.* 54, 6383–6413.
- Abdelnour, F., Genovese, C., Huppert, T., 2010. Hierarchical Bayesian regularization of reconstructions for diffuse optical tomography using multiple priors. *Biomed. Opt. Express* 1, 1084–1103.
- Abler, B., Walter, H., Erk, S., 2005. Neural correlates of frustration. *Neuroreport* 16, 669–672.
- Aksan, N., Goldsmith, H.H., Smider, N.A., Essex, M.J., Clark, R., Hyde, J.S., Klein, M.H., Vandell, D.L., 1999. Derivation and prediction of temperamental types among preschoolers. *Dev. Psychol.* 35, 958–971.
- Aslin, R.N., Mehler, J., 2005. Near-infrared spectroscopy for functional studies of brain activity in human infants: promise, prospects, and challenges. *J. Biomed. Opt.* 10, 11009.
- Blair, C., 2002. School readiness. Integrating cognition and emotion in a neurobiological conceptualization of children's functioning at school entry. *Am. Psychol.* 57, 111–127.
- Blair, K.A., Denham, S.A., Kochanoff, A., Whipple, B., 2004. Playing it cool: temperament, emotion regulation, and social behavior in preschoolers. *J. Sch. Psychol.* 42, 419–443.
- Braungart-Rieker, J.M., Stifter, C.A., 1996. Infants' responses to frustrating situations: continuity and change in reactivity and regulation. *Child Dev.* 67, 1767–1779.
- Calkins, S.D., Dedmon, S.E., Gill, K.L., Lomax, L.E., Johnson, L.M., 2002. Frustration in infancy: implications for emotion regulation, physiological processes, and temperament. *Infancy* 3, 175–197.
- Campbell, S.B., 1995. Behavior problems in preschool children: a review of recent research. *J. Child Psychol. Psychiatry* 36, 113–149.
- Campbell, S.B., Ewing, L.J., 1990. Follow-up of hard-to-manage preschoolers: adjustment at age 9 and predictors of continuing symptoms. *J. Child Psychol. Psychiatry* 31, 871–889.
- Campbell, S.B., Breaux, A.M., Ewing, L.J., Szumowski, E.K., Pierce, E.W., 1986. Parent-identified problem preschoolers: mother-child interaction during play at intake and 1-year follow-up. *J. Abnorm. Child Psychol.* 14, 425–440.
- Carlson, S.M., Wang, T.S., 2007. Inhibitory control and emotion regulation in preschool children. *Cogn. Dev.* 22, 489–510.
- Cole, P.M., 1986. Children's spontaneous control of facial expression. *Child Dev.* 57, 1039–1321.
- Cooper, R.J., Selb, J., Gagnon, L., Phillip, D., Schytz, H.W., Iversen, H.K., Ashina, M., Boas, D.A., 2012. A systematic comparison of motion artifact correction techniques for functional near-infrared spectroscopy. *Front. Neurosci.* 6, 147.
- Cox, R.W., 1996. AFNI: software for analysis and visualization of functional magnetic resonance neuroimages. *Comput. Biomed. Res.* 29, 162–173.
- Custo, A., Wells III, W.M., Barnett, A.H., Hillman, E.M., Boas, D.A., 2006. Effective scattering coefficient of the cerebral spinal fluid in adult head models for diffuse optical imaging. *Appl. Opt.* 45, 4747–4755.
- Delgado, M.R., Nystrom, L.E., Fissell, C., Noll, D.C., Fiez, J.A., 2000. Tracking the hemodynamic responses to reward and punishment in the striatum. *J. Neurophysiol.* 84, 3072–3077.
- Denham, S.A., Caverly, S., Schmidt, M., Blair, K., DeMulder, E., Caal, S., Hamada, H., Mason, T., 2002. Preschool understanding of emotions: contributions to classroom anger and aggression. *J. Child Psychol. Psychiatry* 43, 901–916.
- Denham, S.A., Blair, K.A., DeMulder, E., Levitas, J., Sawyer, K., Auerbach-Major, S., Queenan, P., 2003. Preschool emotional competence: pathway to social competence? *Child Dev.* 74, 238–256.
- Denham, S.A., Bassett, H.H., Way, E., Mincic, M., Zinsser, K., Graling, K., 2012. Preschoolers' emotion knowledge: self-regulatory foundations, and predictions of early school success. *Cogn. Emot.* 26 (4), 667–679.
- Egger, H.L., Erkanli, A., Keeler, G., Potts, E., Walter, B.K., Angold, A., 2006. Test-retest reliability of the Preschool Age Psychiatric Assessment (PAPA). *J. Am. Acad. Child Adolesc. Psychiatry* 45, 538–549.
- Fang, Q., Boas, D.A., 2009. Monte Carlo simulation of photon migration in 3D turbid media accelerated by graphics processing units. *Opt. Express* 17, 20178–20190.
- Friston, K., 2007. *Statistical Parametric Mapping: The Analysis of Functional Brain Images*. Academic, London.
- Gallagher, M., Chiba, A.A., 1996. The amygdala and emotion. *Curr. Opin. Neurobiol.* 6, 221–227.
- Gervain, J., Mehler, J., Werker, J.F., Nelson, C.A., Csibra, G., Lloyd-Fox, S., Shukla, M., Aslin, R.N., 2011. Near-infrared spectroscopy: a report from the McDonnell infant methodology consortium. *Dev. Cogn. Neurosci.* 1, 22–46.
- Giedd, J.N., 2004. Structural magnetic resonance imaging of the adolescent brain. *Ann. N. Y. Acad. Sci.* 1021, 77–85.
- Gogtay, N., Giedd, J.N., Lusk, L., Hayashi, K.M., Greenstein, D., Vaituzis, A.C., Nugent III, T.F., Herman, D.H., Clasen, L.S., Toga, A.W., Rapoport, J.L., Thompson, P.M., 2004. Dynamic mapping of human cortical development during childhood through early adulthood. *Proc. Natl. Acad. Sci. U. S. A.* 101, 8174–8179.
- Gross, J.J., 1998. The emerging field of emotion regulation: an integrative review. *Rev. Gen. Psychol.* 2, 271–299.
- Gusnard, D.A., Akbudak, E., Shulman, G.L., Raichle, M.E., 2001. Medial prefrontal cortex and self-referential mental activity: relation to a default mode of brain function. *Proc. Natl. Acad. Sci. U. S. A.* 98, 4259–4264.
- Heinzel, N., Haeussinger, F.B., Hahn, T., Ehlis, A.C., Plichta, M.M., Fallgatter, A.J., 2013. Variability of (functional) hemodynamics as measured with simultaneous fNIRS and fMRI during intertemporal choice. *Neuroimage* 71C, 125–134.
- Herrmann, M.J., Plichta, M.M., Ehlis, A.C., Fallgatter, A.J., 2005. Optical topography during a Go-NoGo task assessed with multi-channel near-infrared spectroscopy. *Behav. Brain Res.* 160, 135–140.
- Inoue, Y., Sakihara, K., Gunji, A., Ozawa, H., Kimiya, S., Shinoda, H., Kaga, M., Inagaki, M., 2012. Reduced prefrontal hemodynamic response in children with ADHD during the Go/NoGo task: a NIRS study. *Neuroreport* 23, 55–60.
- Knutson, B., Fong, G.W., Adams, C.M., Varner, J.L., Hommer, D., 2001. Dissociation of reward anticipation and outcome with event-related fMRI. *Neuroreport* 12, 3683–3687.
- Mattout, J., Phillips, C., Penny, W.D., Rugg, M.D., Friston, K.J., 2006. MEG source localization under multiple constraints: an extended Bayesian framework. *Neuroimage* 30, 753–767.
- May, J.C., Delgado, M.R., Dahl, R.E., Stenger, V.A., Ryan, N.D., Fiez, J.A., Carter, C.S., 2004. Event-related functional magnetic resonance imaging of reward-related brain circuitry in children and adolescents. *Biol. Psychiatry* 55, 359–366.
- Mitchell, J.P., Banaji, M.R., Macrae, C.N., 2005. The link between social cognition and self-referential thought in the medial prefrontal cortex. *J. Cogn. Neurosci.* 17, 1306–1315.
- Moriguchi, Y., Hiraki, K., 2009. Neural origin of cognitive shifting in young children. *Proc. Natl. Acad. Sci. U. S. A.* 106, 6017–6021.
- Morris, J.S., Frith, C.D., Perrett, D.I., Rowland, D., Young, A.W., Calder, A.J., Dolan, R.J., 1996. A differential neural response in the human amygdala to fearful and happy facial expressions. *Nature* 383, 812–815.
- Perlman, S.B., Pelphrey, K.A., 2010. Regulatory brain development: balancing emotion and cognition. *Soc. Neurosci.* 5 (5–6), 533–542.
- Perlman, S.B., Pelphrey, K.A., 2011. Developing connections for affective regulation: age related changes in emotional brain connectivity. *J. Exp. Child Psychol.* 108 (3), 607–620.
- Pfeifer, J.H., Lieberman, M.D., Dapretto, M., 2007. “I know you are but what am I!?”: neural bases of self- and social knowledge retrieval in children and adults. *J. Cogn. Neurosci.* 19, 1323–1337.
- Rakic, P., Bourgeois, J.P., Goldman-Rakic, P.S., 1994. Synaptic development of the cerebral cortex: implications for learning, memory, and mental illness. *Prog. Brain Res.* 102, 227–243.
- Rothbart, M.K., Derryberry, D., Hershey, K., 2000. Stability of temperament in childhood: laboratory infant assessment to parent report at seven years. In: Molfese, V.J., Molfese, D.L., McCrae, R.R. (Eds.), *Temperament and Personality Development Across the Life Span*. Lawrence Erlbaum Associates, Mahwah, New Jersey, pp. 85–119.
- Rothbart, M.K., Ahadi, S.A., Hershey, K.L., Fisher, P., 2001. Investigations of temperament at three to seven years: the Children's Behavior Questionnaire. *Child Dev.* 72, 1394–1408.
- Saarni, C., 1984. An observational study of children's attempts to monitor their expressive behavior. *Child Dev.* 55, 1504–1513.
- Scholkmann, F., Spichtig, S., Muehleemann, T., Wolf, M., 2010. How to detect and reduce movement artifacts in near-infrared imaging using moving standard deviation and spline interpolation. *Physiol. Meas.* 31, 649–662.
- Schultz, W., Apicella, P., Scarnati, E., Ljungberg, T., 1992. Neuronal activity in monkey ventral striatum related to the expectation of reward. *J. Neurosci.* 12, 4595–4610.
- Siegrist, J., Menrath, I., Stocker, T., Klein, M., Kellermann, T., Shah, N.J., Zilles, K., Schneider, F., 2005. Differential brain activation according to chronic social reward frustration. *Neuroreport* 16, 1899–1903.
- Stifter, C.A., Jain, A., 1996. Psychophysiological correlates of infant temperament: stability of behavior and autonomic patterning from 5 to 18 months. *Dev. Psychobiol.* 29, 379–391.
- Strangman, G., Franceschini, M.A., Boas, D.A., 2003. Factors affecting the accuracy of near-infrared spectroscopy concentration calculations for focal changes in oxygenation parameters. *Neuroimage* 18, 865–879.
- Tzschentke, T.M., 2000. The medial prefrontal cortex as a part of the brain reward system. *Amino Acids* 19, 211–219.

Wakschlag, L.S., Keenan, K., 2001. Clinical significance and correlates of disruptive behavior in environmentally at-risk preschoolers. *J. Clin. Child Psychol.* 30, 262–275.

Wilcox, T., Bortfeld, H., Woods, R., Wruck, E., Boas, D.A., 2005. Using near-infrared spectroscopy to assess neural activation during object processing in infants. *J. Biomed. Opt.* 10, 11010.

Xue, G., Lu, Z., Levin, I.P., Weller, J.A., Li, X., Bechara, A., 2009. Functional dissociations of risk and reward processing in the medial prefrontal cortex. *Cereb. Cortex* 19, 1019–1027.

Ye, J.C., Tak, S., Jang, K.E., Jung, J., Jang, J., 2009. NIRS-SPM: statistical parametric mapping for near-infrared spectroscopy. *Neuroimage* 44, 428–447.